Periodica Polytechnica
Civil Engineering

60(4), pp. 547–560, 2016
DOI: 10.3311/PPci.8545

RESEARCH ARTICLE

New Precast Wall Connection Subjected to Rotational Loading

Hafez Taheri, *Farzad* Hejazi, *Ramin* Vaghei, *Mohd Saleh* Jaafar, *Abang Abdullah Aabang* Ali

Received 05-09-2015, revised 16-12-2015, accepted 15-01-2016

Abstract

The connection of discrete elements in precast concrete structures has important role in overall continuity of the building. Investigations show that most precast structure damages occur in connections under earthquake loads or other disasters. This study aims to propose a new connection in order to improve rotational loading capacity and develop a finite element model of precast wall with connections by considering all details of different parts for a contemporary connection, as well as the proposed connection. Pushover analysis is conducted for major or minor bending moment and torsion moment degrees of freedom (DOFs) to obtain the capacity of each type of connection. Four key features of concrete panels and steel reinforcements are considered to determine the effect of incremental lateral movements. Pushover results indicate a significant improvement in the maximum flexural strength of the proposed connection. Indeed, the maximum moment in the bending moment DOF is enhanced when the proposed connection is used. Consequently, the result reveals that the contemporary connection has a significant defect in terms of strength in bending moment and torsion moment DOFs.

Keywords

Industrial building systems · Precast concrete structures · Wall connection · Monotonic Loading · Pushover analysis · Finite element analysis

Hafez Taheri

Civil Engineering Department, Faculty of Engineering, Universiti Putra Malaysia, UPM, 43400, Serdang, Selangor, Darul Ehsan, Malaysia

Farzad Hejazi

Civil Engineering Department, Faculty of Engineering, Universiti Putra Malaysia, UPM, 43400, Serdang, Selangor, Darul Ehsan, Malaysia
e-mail: farzad@upm.edu.my

Ramin Vaghei

Mohd Saleh Jaafar

Civil Engineering Department, Faculty of Engineering, Universiti Putra Malaysia, UPM, 43400, Serdang, Selangor, Darul Ehsan, Malaysia

Abang Abdullah Aabang Ali

Housing Reseach Centre, Faculty of Engineering, Universiti Putra Malaysia, UPM, 43400, Serdang, Selangor, Darul Ehsan, Malaysia

1 Introduction

The rate of construction serves a key function in the final cost of a project. Therefore, Industrialized Building Systems (IBSs) are developed in some countries to implement a project at the minimum time and best speed. In some countries like Malaysia, this term is extensively used to refer to a method of construction in which the elements of structure are produced in a controlled environment and transported to the site location and installed in their main locations. In other countries, this term is known as Open Building Systems and Modular Coordination [1]. However, the concept of all definitions is similar. Many studies have investigated the use of precast concrete structures rather than in situ concrete structures. The amount of savings in labor and material, enhanced product quality and workmanship, and rate of construction have resulted in the spread of marketing in this industry over the past half century [2].

An important aspect of design for precast structures is connection. A connection should ensure the overall continuity of a structure and should have suitable ductility and rigidity. Therefore, the design and development of mechanical connection devices, especially the so-called fail-safe connections, have been considered in recent years. These connections could guarantee the continuity of the structure [2]. In fact, the connection in precast concrete structure should emulate the behavior of an in situ connection in terms of strength and continuity. The concept of emulative detailing is well defined in the American Concrete Institute Committee 550 guide report as “the design of connection systems in a precast concrete structure so that its structural performance is equivalent to that of a conventionally designed cast-in-place, monolithic concrete structure” [3]. Therefore, when the connection behavior of concrete panels and steel reinforcements in precast concrete structure is more similar to that of in situ connection, the system shows better performance in terms of continuity and integration [4].

The literature shows that the main obstacle to the improvement of precast concrete is the integration of connections between members. Thus, the precast load-bearing connections should be reliable and durable throughout its service life. Clough and Engineers [5] reported that precast concrete build-

ings are exposed to less rigidity than cast in situ buildings because of the lack of continuity. As such, special consideration of ductility and redundancy should be integrated into the design process to increase the serviceability of precast concrete structures in seismic regions, as well as to decrease cost. The function of connections is more vital in prefabricated walls. Actually, prefabricated load-bearing wall panels are structurally efficient members and economical means of transferring loads from the diaphragm and roof to the foundation. These functions of prefabricated load-bearing wall panels result in their extensive use and low cost [6]. Thus, eliminating obstacles and providing sufficient strength and ductility for precast load-bearing connections enable contractors to use precast concrete structures and profit from their advantages.

Depending on the number of members that connect to each other, different types of connections can generally be obtained. For connecting beam to column, two types of joints are extensively used. In the first type, embedded steel plates are placed in molds and then casted in concrete. Therefore, with the use of these plates, precast members can be connected by welding and bolting. Wet concrete is used for fireproofing of connections. Bhatt and Kirk [7] and Choi, Choi, and Choi [8] reported on this type of joint. In the second type, wet concrete is used mostly for connecting precast members and casting in situ concrete. These types of joints are well known because of minimum site work, such as welding and bolting. Khoo, Li, and Yip [9], Xue and Yang [10], Khaloo and Parastesh [11], and Parastesh, Hajirasouliha, and Ramezani [12] have studied this type of joint. Diaphragms are another member of precast concrete structures that are extensively used in transferring and carrying load. Different connectors are designed for floor and diaphragms to resist compression and tension forces at boundary edges and shear forces between diaphragms at mid-spans without detaching. In addition to mechanical connectors, wet concrete is also used for joining them. Other types of connections used for floor and diaphragms have been investigated by researchers [13–17].

Precast concrete wall systems also have different types of connections. In the past, one of the most well-known members that is extensively used in high-rise buildings is precast load-bearing shear wall panels. Precast concrete shear wall systems include all elements needed to transmit lateral seismic force between the foundation and a roof diaphragm. Precast concrete shear wall systems are well known because of good control of concrete quality of precast walls and ease of erection and installation at the site [18]. Experimental studies and literature on different shapes of connections for precast concrete walls included facades, cladding, and shear walls [19–21]. Over time, new materials are also investigated for connections in precast members, especially walls. For example, CFRP composite connector is the loop connection for linking precast concrete members, such as wall panels or floor system [22]. However, after all improvements in terms of the design of connections for precast concrete walls, most studies have reported that the main problem is the integration of connections between members. Therefore, special consideration of ductility and redundancy must be set in the design process for precast wall systems to increase the serviceability of precast concrete structures in seismic regions, as well as to decrease the cost. Thus, more studies were conducted to investigate the behavior of precast wall connections in seismic zones [23–27].

The joints in precast concrete walls are divided in two groups. The first group includes vertical joints that act as coupling media between the panels. Their behavior is similar to spandrel beams in buildings. Shear key connection is categorized under this group. Chakrabarti, Nayak, and Paul [28] and Foerster et al., [18] have investigated the characteristics of this joint. The second group includes horizontal joints at the floor levels. Horizontal joints are stiffer than vertical joints because of normal pressure due to the weight of the wall panel and other dead loads on the joint. In this group, splice sleeves are more popular. Splice sleeves consist of Lenton Interlok and NMB Splice Sleeve [29].

Loop connection is also a type of connection used to connect precast walls and beams. Given the simplicity of this connection, the loop connection is extensively used by contractors. In this connection, the full 180°hooks or projecting bars overlap each other and the transverse reinforcements should pass through the hook bars to prevent brittle failure. The loop connection is a wet connection and needs concrete in place of joint. Recently, some studies investigated and tested the behavior of loop connection under different loading situations [30–33].

A review of the literature reveals many types of connections for precast structures. However, the use of each connection in IBS has its limitations. Some connections are impractical and expensive that clients cannot be easily convinced to use them. For most of these connections, academic studies in terms of strength, ductility, energy dissipation, and dynamic loading are insufficient. Therefore, the expansion of this area of knowledge with respect to the trend of contractors to precast structures is inevitable. The main aim of this study is to develop a 3D realistic finite element model to assess the effectiveness of connections on reinforced concrete frame structures against the imposing load.

2 Precast Wall Connections

A connection should ensure the overall continuity of the structure and should have suitable ductility and rigidity. For precast concrete structures, considering a suitable connection is more important than considering ordinary structures. The connections for precast concrete walls are vital when they carry vertical and lateral loads. These connections should be capable of transferring the load to another member of the structure and finally to the foundation of the building. Appreciated connection among walls guarantees the transfer of the conducting load from one wall to the adjacent wall. Thus, these two walls work together. This connection should possess sufficient strength to carry loads and sufficient ductility.

These walls are used as exterior or interior walls of buildings, walls of lift cores, and parapets. These walls are used not only on apartments and hotels with medium height but also on ordinary flats and homes with low height. Given that precast walls are produced in plants, the strength of concrete is determined and controlled accurately. The finished surface is relatively smooth that the walls are immediately ready for painting or wallpaper.

2.1 Loop connection

The details of loop connection are shown in Fig. 1. The model comprises two concrete wall panels, concrete reinforcing welded mesh (BRC), hooks, main middle bar, and in situ concrete. The loop connection is provided by anchor bars or loops from reinforcing bars anchored by grouting in recesses and cores. The joint is filled with joint concrete or grout.

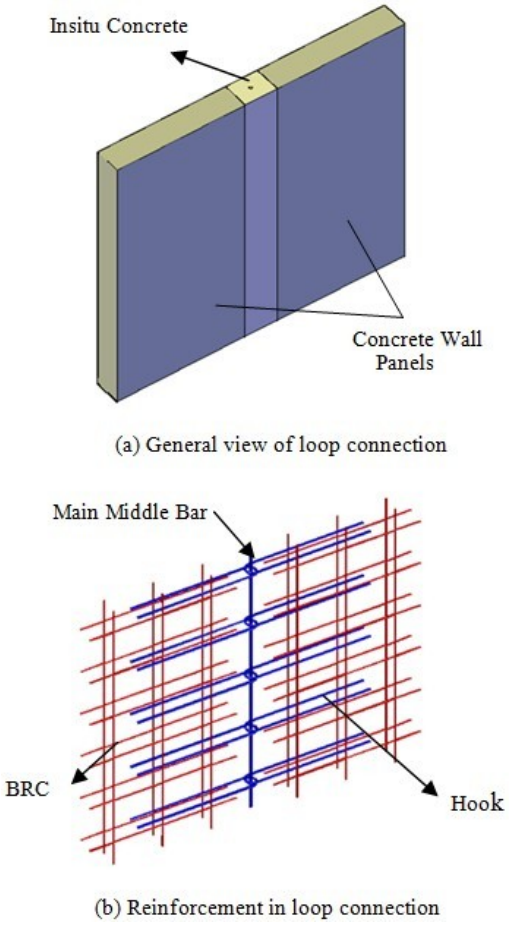

Fig. 1. Details of loop connection

Loop connection is used among concrete wall panels with required continuity. However, production is difficult because of the projecting bars. Loop connections for precast walls in IBS buildings are generally designed based on numerical and experimental studies. In addition, these loop connections are designed to resist static axial force in plane compression. Moreover, the loop connection cannot provide sufficient strength for other degrees of freedom (DOFs; e.g., out-of-plane loadings). Thus, the structural components do not provide the integrity required to resist lateral dynamic loading in all directions when this type of connection is used. Most existing connections are also highly dependent on the ability of workers to sporadically set the costly and time-consuming connections. In this study, we developed a new connection for precast walls to compensate for the connection problems and to provide sufficient strength for wall joints in all directions (i.e., 6 DOF). Time and cost are the two main parameters in setting and fabricating the connections. The proposed connection aims to improve the desired integrity for structural components in any direction and to protect the structures against multisupport excitations.

2.2 Proposed Connection

The proposed connection is composed of male and female panels and channels, rubber, BRC reinforcements, hooks, screw, and nut. The parts of the proposed connection and the reinforcement and loop locations are shown in Fig. 2.

The multidirectional resistances of the proposed connection are based on 6 DOFs. Axial and shear forces, torsion, and bending moments are the DOFs considered in the proposed connection design. The following solutions are directed at a 3D proposed connection and are not limited to any particular size or configuration.

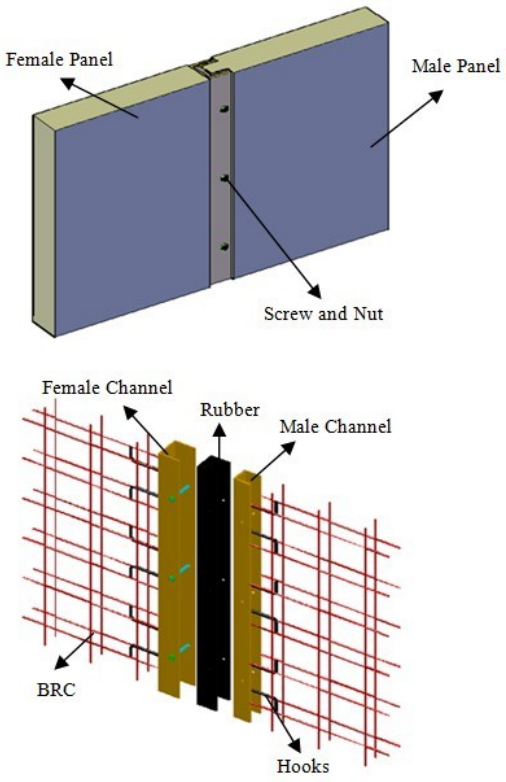

Fig. 2. Details of proposed connection

3 Development of Finite Element Model

In this study, a 3D actual model was developed to investigate the effect of lateral loads on precast walls. The loop and proposed connections were simulated based on the finite element method using the Abaqus software. The loop connection is a

contemporary connection that is extensively used in IBS structures. However, a new connection (proposed connection) was designed and developed to improve the strength and ductility of precast wall connections.

3.1 Components of Proposed Connection

Fig. 2 shows the different parts of the proposed connection, namely, male panel, female panel, male channel, female channel, rubber, BRC, hooks, screw, and nut. The reinforcement and hooks are also shown in the figure.

3.1.1 Concrete Wall Panel

The dimensions of concrete wall panels are shown in Fig. 3. A ridge at the end of the male panel has been generated to interlock the male and female panels. All these parts are modeled as solid parts.

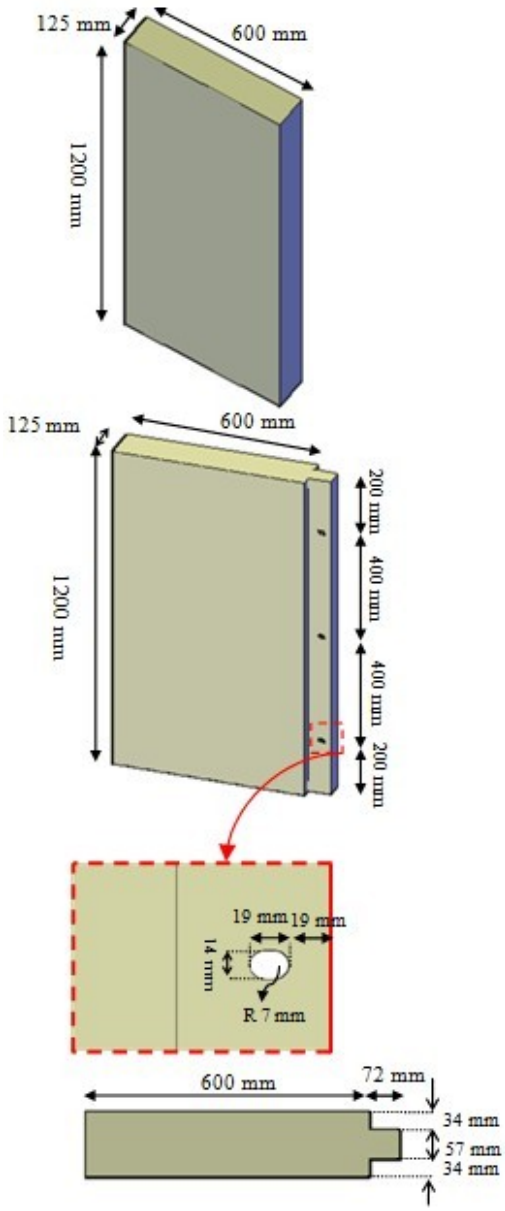

Fig. 3. Details and dimensions of concrete wall panels in proposed connection

3.1.2 BRC

The arrangement of BRC-A7 is shown in Fig. 4. The center to center distance of two layers of BRC is 65 mm. For each net of the BRC, the diameter of the bars is 7 mm and the distance of the bars is 200 mm in the vertical and horizontal directions.

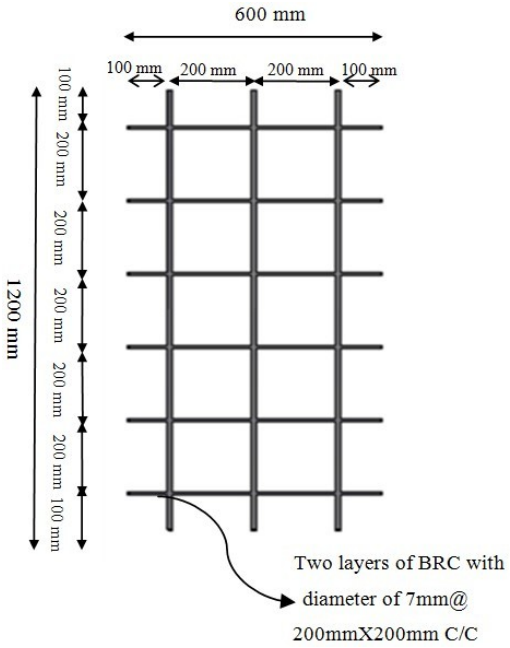

Fig. 4. BRC dimensions and details (mm).

3.1.3 U-Shaped steel channel (Female Channel and Male Channel) and U-Shaped Rubber

For the U-shaped steel channel and U-shaped rubber, the thickness of the flanges and webs is 8 mm. These parts are generated as solid parts in the Abaqus software. Both flanges have three holes, as shown in Fig. 5(a). This figure also shows the common and parametric dimensions of the U-shaped steel channel and U-shaped rubber. The values of all these dimensions are listed in Table 1. The cross-sections and detailed dimensions of the male channel, rubber, and female channel are shown in Figs. 5(b), 5(c), and 5(d), respectively.

3.1.4 Hooks

Three hooks, with dimensions shown in Fig. 6, are welded to the U-shaped steel channels in the proposed connection. The function of these hooks is to bond the U-shaped steel channels to the concrete panels to prevent sliding between them. The diameter of the hooks is 12 mm. The hooks are welded to the steel channels before placing them in molds and casting in concrete.

3.1.5 Screw and nut

The screw and nut are used to attach the U-shaped steel channels and U-shaped rubber to the concrete panels. The hole diameter of the screw and nut is 12 mm. However, considering tolerance, the hole diameter of the flanges and male concrete panel is 14 mm. The details of the screw and nut are shown in Fig. 7.

Tab. 1. Parametric Values

Dimension	Height (mm)	Web-t (mm)	Flange-t (mm)	Web-L (mm)	Flange-L (mm)	X (mm)
Female Channel	1200	8	8	105	90	28
Male Channel	1200	8	8	73	80	34
Rubber	1200	8	8	89	75	21

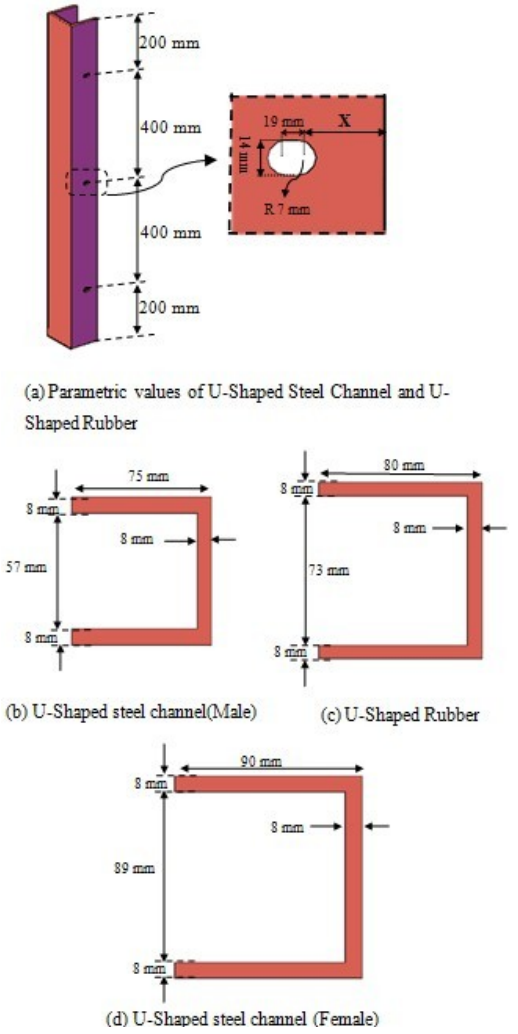

Fig. 5. Details and Dimensions of Female channel, Male channel and Rubber in proposed connection

3.2 Components of Loop Connection

As shown in Fig. 8, the loop connection consists of two concrete wall panels, BRC, hooks, main middle bar, and in situ concrete.

In the loop connection, the full 180°hooks are embedded as reinforcement before concreting the molds of concrete wall panels. These hooks protrude on one side of the concrete wall panel to cover other hooks from another concrete wall panel. Moreover, the main middle bar with 12 mm diameter passes through the hooks to generate the loop connection and wet concrete is poured in place of the connection. Fig. 8 shows the dimensions of the loop connection generated in this study.

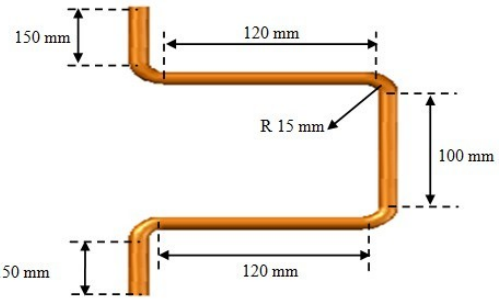

Fig. 6. Hooks dimensions and details (mm)

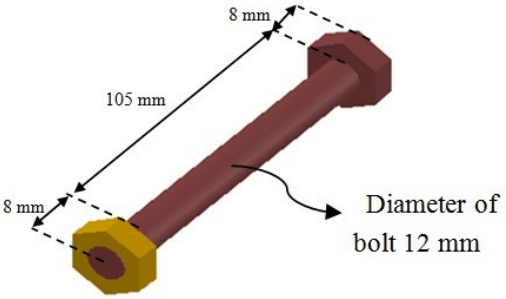

Fig. 7. Details and dimensions of Rubber channel, screw and nut

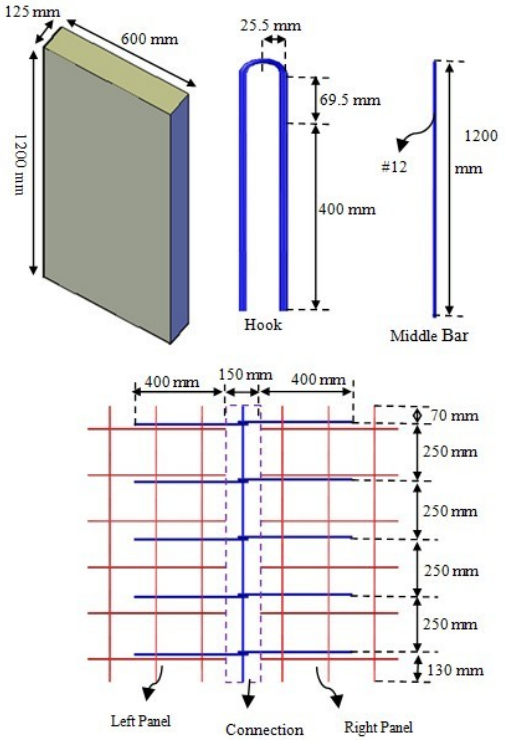

Fig. 8. Concrete wall panels in loop Connection (mm)

3.3 Property of Materials

The properties of all the materials used in this study are described as follows:

3.3.1 Steel Properties

The properties of steel materials for the loop and proposed connections are defined as follows:

The values related to the stress–strain relationship of steel are listed in Table 2. Based on this table, the plastic behavior of steel is defined as linear.

3.3.2 Concrete Properties

The properties of grade B50 concrete are listed Table 3 for the loop and proposed connections. The mass density of concrete is 2,400 kg/m^3. The plastic behavior of concrete is modeled based on concrete damage plasticity theory.

3.3.3 Rubber Properties

The behavior of U-shaped rubber between steel channels in the proposed connection and the values of three types of test data, namely, uniaxial, biaxial, and planar test data, are listed in Table 4. This rubber is modeled as a hyperelastic material with a mass density of 1,200 kg/m^3 in Abaqus software.

3.4 Interactions

3.4.1 Loop connections Interactions

In the loop connection, the surface to surface interaction is used for the contact surface of concrete wall panels and the middle in situ concrete. Moreover, the constraint between all reinforcements and concrete wall panels is embedded constraint.

3.4.2 Proposed Connection Interactions

In the proposed connection, the surface to surface interaction is used for the contact surface of rubber and steel channels, as well as the outer surface of bolts and inner surface of holes in steel channels, rubber, and concrete. Tie constraint is used for binding the steel channels to concrete of female and male panels. Moreover, the inner surface of nuts is tied to the outer surface of bolts. Similar to the loop connection, all reinforcements and hooks are also embedded in the concrete wall panels.

3.5 Load and Boundary Conditions

For each DOF, the position of the loads and boundary conditions is different. However, for moment DOF, the boundary condition of all wall panels and connections at the bottom is selected as the fixed boundary condition. Only the location and direction of the concentrated load is changed to generate different moment DOFs. Fig. 9 and Fig. 10 show the locations of the applied concentrated forces in DOFs, namely, URx (rotation about the X-axis), URy (rotation about the Y-axis), and URz (rotation about the Z-axis), in the loop and proposed connections.

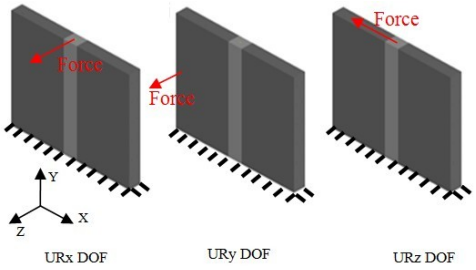

Fig. 9. Boundary condition and loading in URx, URy, URz degree of freedoms in Loop connection.

This type of loading is used for generating the moment around the three main coordinate systems. These DOFs are analyzed only for monotonic loading.

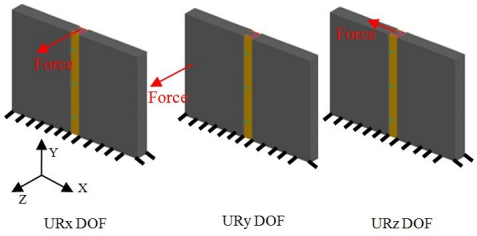

Fig. 10. Boundary condition and loading in URx, URy, URz degree of freedoms in Proposed connection.

The time–load factor relationship for monotonic loading is shown in Fig. 11. The magnitude of loading is 5,000 N.

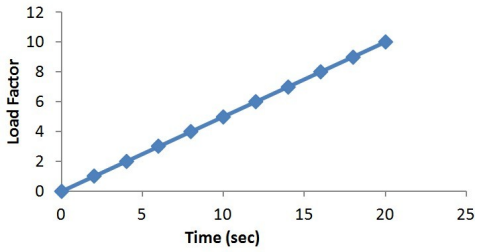

Fig. 11. Monotonic loading for URx, URy, URz degree of freedoms.

3.6 Meshing

Two methods of meshing, namely, structured and sweep, are used to mesh all parts of the loop and proposed connections. As shown in Fig. 12, reinforcements and hooks in the loop and proposed connections are meshed as wire. The T3D2 element type is used for meshing. However, for concrete panels, the eight-node linear brick element with reduced integration (C3D8R) is selected for meshing.

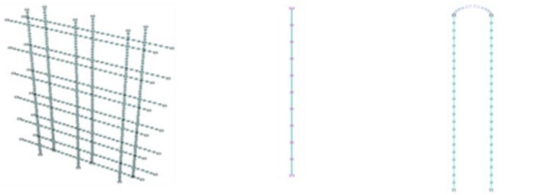

(a) BRC meshing. (b) Main middle bar meshing (c) Hook meshing

Fig. 12. Reinforcement meshing.

Tab. 2. Stress-strain relationship for steel

Mass Density	Young's Modulus	Poisson's Ratio	Yield Stress	Plastic Strain
7850 kg/m^3	196000 N/mm^2	0.3	240	0
			370	0.25

Tab. 3. The material parameters of CDP model for concrete class B50. [34]

Material's parameters	parameters	The parameters Material's of CDP model	
		β	38^o
Concrete elasticity		m	1
E[GPa]	19.7	$f = f_{b0} / f_c$	1.12
ν	0.19	γ	0.666
Concrete compression hardening		Concrete compression damage	
Stress [MPa]	Crushing strain [-]	DamageC [-]	Crushing strain [-]
15	0	0	0
20.197	7.47 E-05	0	7.47 E-05
30.00061	9.88 E-05	0	9.88 E-05
40.30378	0.000154	0	0.000154
50.00769	0.000762	0	0.000762
40.23609	0.002558	0.195402	0.002558
20.23609	0.005675	0.596382	0.005675
5.257557	0.011733	0.894865	0.011733
Concrete tension stiffening		Concrete tension damage	
Stress [MPa]	Cracking strain [-]	DamageT [-]	Cracking strain [-]
1.9989			
2.84	3.33E-05		3.33E-05
1.8698	0.0001	0.406411	0.0001
0.862723	0.0002	0.6963	0.0002
0.226254	0.000685	0.920389	0.000685
0.056576	0.001087	0.980093	0.001087

Tab. 4. Property of rubber based on the data of three tests (based on the Abaqus documentation)

Uniaxial Test Data		Biaxial Test Data		Planar Test Data	
Nominal Stress (MPa)	Nominal Strain	Nominal Stress (MPa)	Nominal Strain	Nominal Stress (MPa)	Nominal Strain
1.5506	0.1338	0.9384	0.02	0.6	0.069
2.4367	0.2675	1.59	0.06	1.6	0.1034
3.1013	0.3567	2.4087	0.11	2.4	0.1724
4.2089	0.6242	2.622	0.14	3.36	0.2828
5.3165	0.8917	3.324	0.2	4.2	0.4276
5.981	1.1592	4.4278	0.31	6	0.8483
6.8671	1.4268	5.183	0.42	7.8	1.3862
8.8608	2.051	6.6024	0.68	9.6	2
10.6329	2.586	7.7794	0.94	11.12	2.4897
12.4051	3.0318	9.7857	1.49	12.96	3.0345
16.1709	3.7898	12.6351	2.03	14.88	3.4483
19.9367	4.3694	14.6804	2.43	16.58	3.7793
23.481	4.8153	17.4	2.75	18.2	4.0621
27.4684	5.172	20.1058	3.07		
31.0127	5.4395	22.4502	3.26		
34.557	5.707	24.653	3.45		
38.3228	5.9299				
42.0886	6.0637				
45.6329	6.1975				
49.3987	6.3312				
53.1646	6.465				
56.9304	6.5541				
64.2405	6.6433				

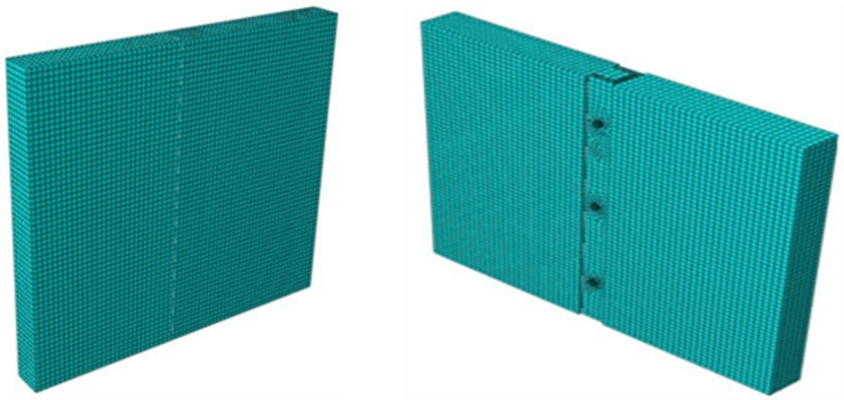

Fig. 13. Reinforcement meshing.

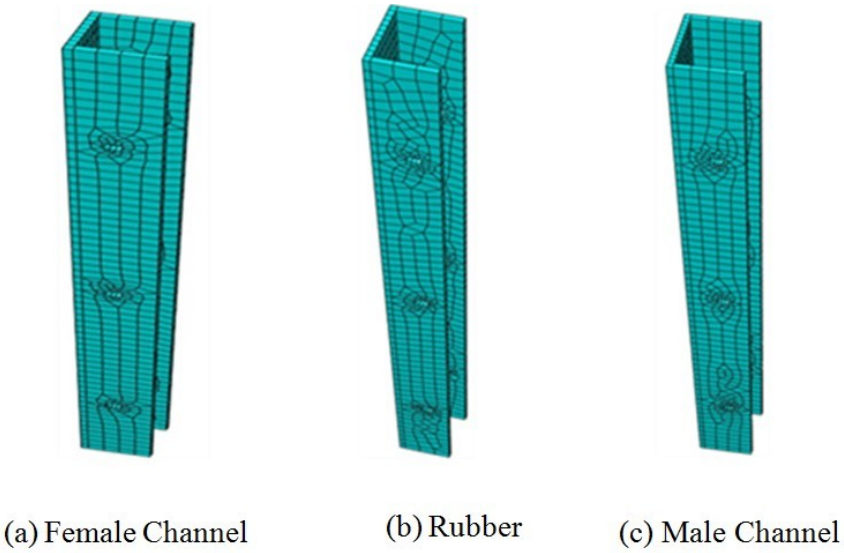

Fig. 14. Steel channels and rubber meshing

For concrete wall panels, the structured technique is used. For the ridge of the concrete male panel in the proposed connection, the ridge is separated by a partition and meshed using sweep technique because of the holes (Fig. 13)

For the steel channels and rubber, two meshing techniques are used. First, for the web, the structured technique is implemented. Second, for the flanges of the U-shaped steel channels and rubber, the sweep technique is implemented. C3D8R is also selected for meshing, as shown in Fig. 14.

Fig. 15 shows the meshing of bolts and nuts using the sweep method and the C3D8R element type.

Therefore, with the development of 3D realistic finite element model in this stage, assessing the effectiveness and behavior of the loop and proposed connections on the structure frame subjected to lateral loads is possible.

4 Results and Discussion

The contribution of connections subjected to monotonic loading is investigated in this section. A total of 12 monotonic simulations were conducted in this study, including 6 models of axial force, major or minor shear force, and major or minor bending moment and torsion moment DOFs for the loop connection and 6 DOFs for the proposed connection. The complete results for each monotonic simulation are shown in the figures. Graphs of the load–relative displacement curve are also provided. As described in the model, relative displacements were implemented based on the adjacent concrete panels and graphs were drawn using the same procedure to reveal the real contribution of connections.

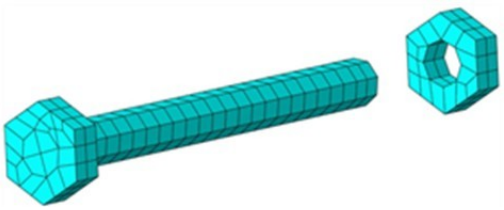

Fig. 15. Screw and nut meshing.

The two data sets for each connection were averaged to determine the load–displacement values. The graph reveals that the performance of the wall is dependent on the connection material and its corresponding material properties. Each connection material reaches its maximum strength at a different load

and fails at a different load and displacement. Therefore, considering several different parameters when analyzing the various connection materials is important. The wall connections in this study typically fail when precast walls either have many cracks or are crushed when the ultimate strength of concrete is achieved. Thus, the connection is no longer effectively attached to the wall and the wall is unable to resist any further forces.

The connection section geometry and material properties are considered the same in the examples to compare the responses of the common and proposed connections. The base shear versus maximum relative displacement of the loop and proposed connections for different DOFs are plotted. Afterward, the results are compared.

A numerical analysis is conducted to investigate the effect of lateral displacements on the response of precast wall to wall connection. Five key features, including capacity, maximum principal stress, deformation, absolute plastic strain (PEMAG), and concrete damage, of the concrete panels and steel reinforcements are considered to determine the effect of the incremental lateral movements.

4.1 Pushover Capacity

4.1.1 Capacity to torsion moment (fourth DOF)

In the fourth DOF, the maximum rotation versus bending moment at the base is calculated and shown in Fig. 16.

This DOF refers to the in-plane moment, which results in torsion. In contrast to the loop connection, the proposed connection exhibits better performance in accordance with the maximum bending moment. The maximum bending moment is equal to 10.810 kN·m for the loop connection. However, the maximum bending moment is improved to 11.380 kN·m for the proposed connection in the fourth DOF.

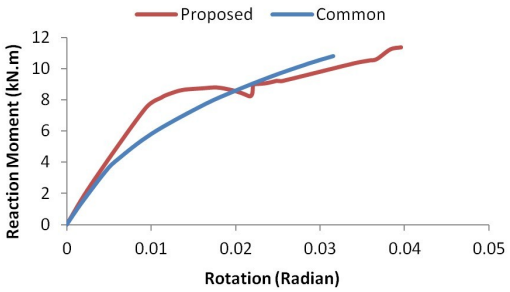

Fig. 16. Pushover Analysis of Common/Proposed connection subjected to Monotonic Loading for the 4th Degree of Freedom.

The curve shows that the capacity of the loop connection in the fourth DOF improved to approximately 45% using the proposed connection. Table 5 shows the capacity of each connection and the amount of improvement by the proposed connection.

4.1.2 Capacity to minor bending moment (fifth DOF)

The maximum rotation versus bending moment at the base, which is the out-of-plane moment in the fifth DOF is calculated and shown in Fig. 17. After drawing the rotation versus bending moment curve, the maximum bending moment that applies to the connections is obtained. Therefore, the maximum bending moment for the loop connection is 12.460 kN·m and for the proposed connection is 18.180 kN·m.

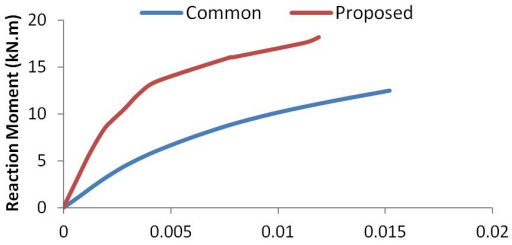

Fig. 17. Pushover Analysis of Common/Proposed connection subjected to Monotonic Loading for the 5th Degree of Freedom.

The results of the calculations related to the moment–rotation graph are shown in Table 6. We conclude that in 5th DOF, the proposed connection increases the capacity by 160% rather than the loop connection.

4.1.3 Capacity to Major bending moment (sixth DOF)

The out-of-plane moment in the sixth DOF in the form of the maximum rotation versus bending moment at the base is calculated and shown in Fig. 18. Similar to fourth and fifth DOFs, the maximum bending moments for connections are obtained from the rotation versus reaction moment curve. The maximum bending moment for the loop connection is approximately 9.964 kN·m. However, in the loop connection, the corresponding value is improved significantly to 37.280 kN·m, as shown in Fig. 18.

As shown in Table 7, the improvement of capacity by the proposed connection rather than loop connection is approximately 298.78%.

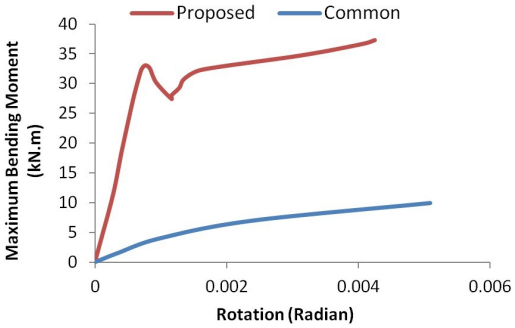

Fig. 18. Pushover Analysis of Common/Proposed connection subjected to Monotonic Loading for the 6th Degree of Freedom.

4.2 Stress distribution

4.2.1 Stress distribution to the torsion moment (fourth DOF)

In the loop connection of the fourth DOF, stress is distributed along the middle in situ concrete connection, as shown in Fig. 19. This figure shows that reinforcement of the plastic range of the stress–strain curve and concrete reaches its ultimate

Tab. 5. Capacity of the Common/Proposed connections in 4th DOF

CONNECTIONS	Area Under of Moment Vs Rotation Graph (kN.m)
Loop connection	0.219
Proposed Connection	0.319
Difference Value	0.1
Capacity Improvement (%)	45.7%

Tab. 6. Capacity of the Common/Proposed connections in 5th DOF

CONNECTIONS	Area Under of Moment Vs Rotation Graph (kN.m)
Loop connection	0.120
Proposed Connection	0.312
Difference Value	0.192
Capacity Improvement (%)	160 %

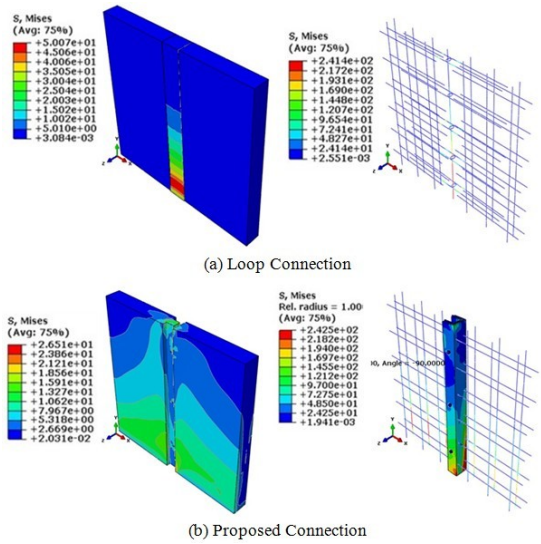

Fig. 19. Stress Results for 4th Degree of Freedom

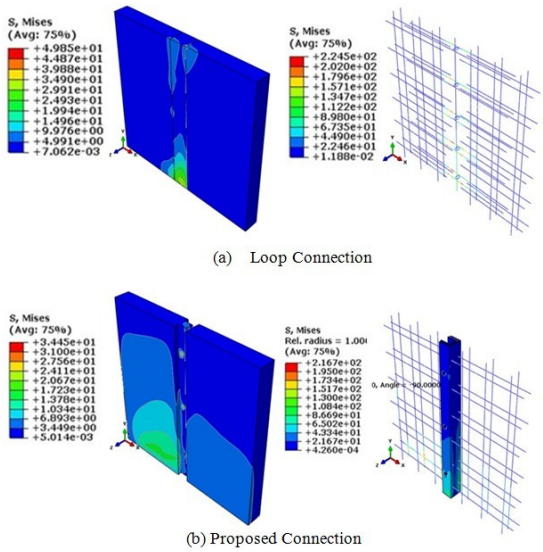

Fig. 20. Stress Results for 5th Degree of Freedom

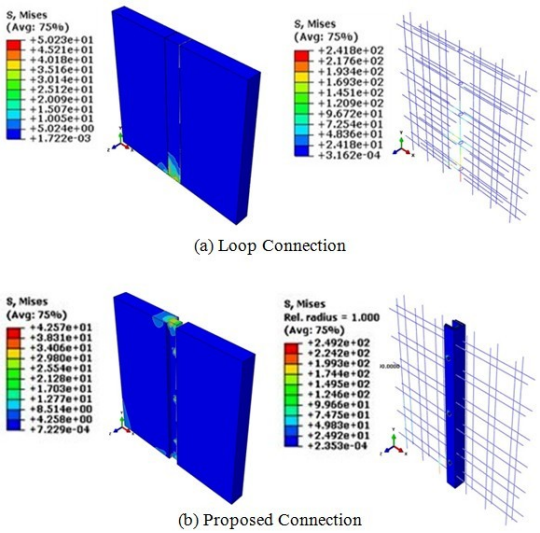

Fig. 21. Stress Results for 6th Degree of Freedom

strength. However, as shown in Fig. 19, concrete in the proposed connection did not reach its ultimate strength.

4.2.2 Stress distribution to the minor bending moment (fifth DOF)

As shown in Fig. 20, the reinforcements remain elastic in the loop and proposed connections in association with the yield stress for steel material, which is assumed to be 240 MPa. Based on these values, we conclude that, in the loop connection, stress of concrete approximately reaches its ultimate strength, but the ultimate strength of concrete in the proposed connection is less than the ultimate strength of concrete. Moreover, reinforcement in both connections does not yield. Actually, in the proposed connection, high damage in panels causes the decrease in the bearing capacity of concrete and hinders concrete from achieving its ultimate strength.

4.2.3 Stress distribution to the major bending moment (sixth DOF)

For the sixth DOF, in both aforementioned connections, reinforcement of the plastic range of the stress–strain curve is in accordance with the stress limit state, as shown in Fig. 21. How-

Tab. 7. Capacity of the Common/Proposed connections in 6th DOF

CONNECTIONS	Area Under of Moment Vs Rotation Graph (kN.m)
Loop connection	32.6e-3
Proposed Connection	0.130
Difference Value	97.4e-3
Capacity Improvement (%)	298.78 %

ever, for the loop connection, concrete reaches the maximum stress, by contrast, the maximum stress in the proposed connection is 42.57 MPa.

4.3 Displacement distribution

4.3.1 Displacement distribution to the torsion moment (fourth DOF)

The displacement for both types of connections is high at the top of the panels and low at the bottom of the panels. The reinforcements and concrete in the loop connection have the same displacement value of approximately 45 mm, which is shown in Fig. 22. However, these values vary from 12.94 mm for concrete to 37.4 mm for reinforcements in the proposed connection. This difference is due to the existence of rubber, therefore resulting in the easy movement of channels.

4.3.2 Displacement distribution to the minor bending moment (fifth DOF)

The pattern of distribution of displacement is exactly the same for both connections. The maximum displacement occurs at the corners and top of the left panel. The value of displacement in the loop connection is approximately two times that in the proposed connection. Fig. 23 shows the amount of deformation in concrete in both types of connections.

4.3.3 Displacement distribution to the major bending moment (sixth DOF)

As shown in Fig. 24, the maximum displacement in the sixth DOF occurs at the corners and top of the panels. Indeed, the deformation of panels in the loop connection is significantly higher than that in the proposed connection. In the proposed connection, the right panel has approximately zero displacement for the concrete and reinforcements. This finding indicates that the imposing load cannot move the right panel. It is assumed that greater imposing loads affect rubber and pass through it to generate displacement in the right panel.

4.4 Damage in tension

4.4.1 Damage in tension to the torsion moment (fourth DOF)

The contours in Fig. 25 show that the magnitude of damage in tension (DAMAGE_T) is the same for both types of connections. However, the distribution of the cracks is totally different. In the loop connection, most of the cracks are formed at the bottom of the middle in situ concrete connection. However, for the proposed connection, most of the cracks are formed at the bottom of both panels because the integration of connections has a good correlation with the adjacent precast concrete panels in the proposed connection. However, this integrity cannot meet the requirements. In fact, the proposed connection leads to the detection of the maximum capacity of precast walls caused by the spread of tension damage throughout of the panels.

4.4.2 Damage in tension to the minor bending moment (fifth DOF)

Fig. 26 represents the distribution of cracks caused by tension damage in the concrete panels. Notably, in the proposed connection, cracks spread on the walls more significantly in contrast to the loop connection. We conclude that the proposed connection contributes more to the bearing tension loads from the panels.

Integration of connections in the proposed connection shows a good correlation with adjacent precast concrete panels. However, the lack of integration in the loop connection results in concentrated stress instead of spreading it to expand the capacity.

4.4.3 Damage in tension to the major bending moment (sixth DOF)

The maximum tension damage (DAMAGE_T), based on Fig. 27, is 9.801e−1. Many cracks due to tension are created at the bottom of the middle in situ concrete connection in the loop connection. Damage attributed to tension in the proposed connection is also formed around the bolts and at the bottom and right corners of the male panel, which shows the contribution of rubber in the distribution of damage regardless of the value.

5 Conclusions

In this study, we propose a new type of connection (i.e., U-shaped steel channel) for precast walls. This connection is subjected to monotonic loading. The performances of the loop and proposed connections are compared to verify the efficiency, high resistance function, and proper action against multidirectional progressive force of the proposed connections. Finite element analysis is further utilized to investigate the capacity behavior of the U-shaped steel channel connection.

Pushover results indicate that the maximum moment of the loop connection in the fourth, fifth, and sixth DOFs are enhanced by 45%, 160%, and 298.78% and increased from 0.219 kN·m, 0.120 kN·m, and $32.6e^{-3}$ kN·m to 0.319 kN·m, 0.312 kN·m, and 0.130 kN·m, respectively.

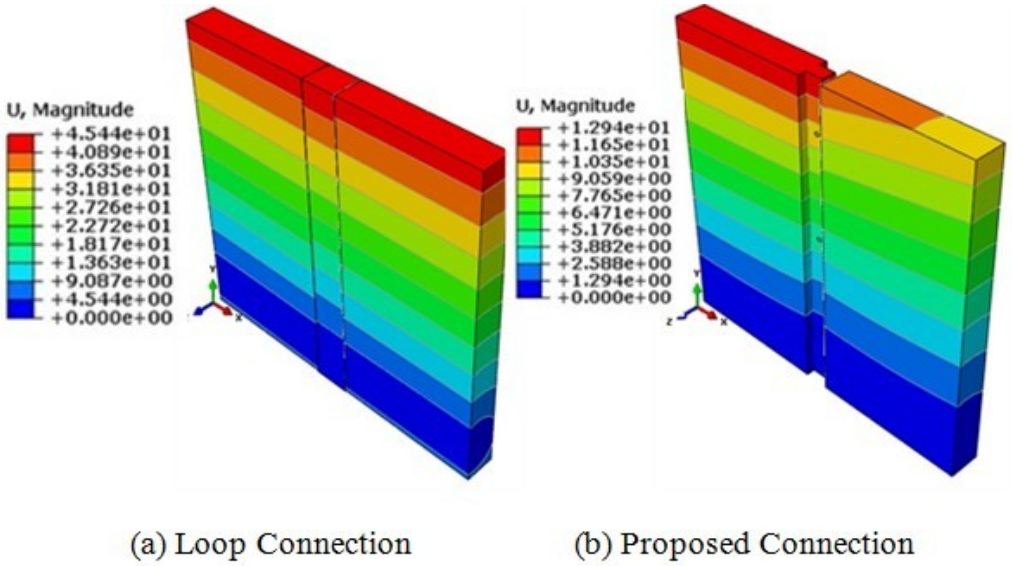

Fig. 22. Displacement Results for 4th Degree of Freedom

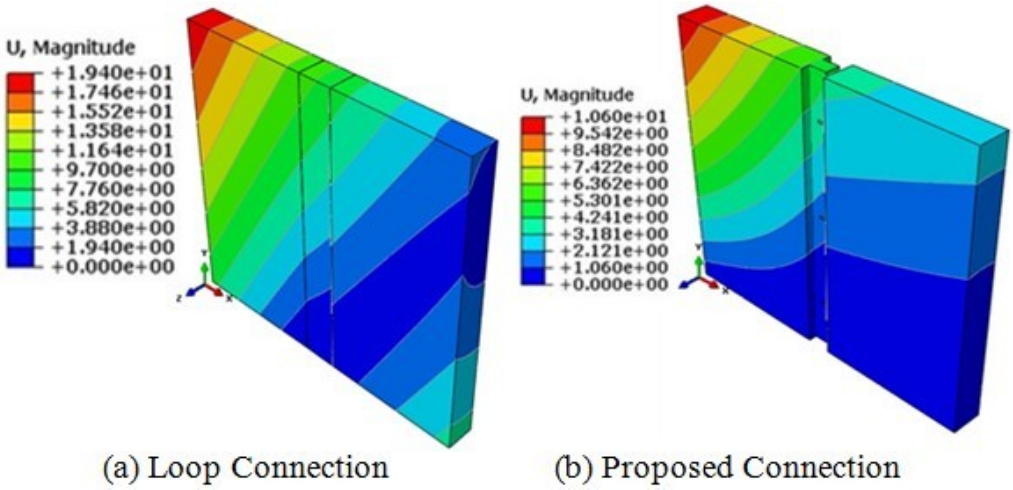

Fig. 23. Displacement Results for 5th Degree of Freedom

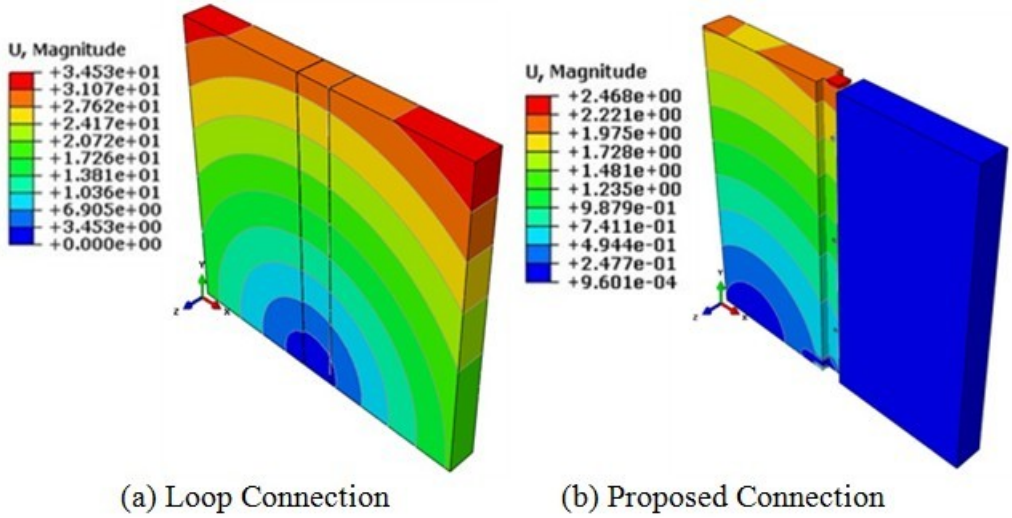

Fig. 24. Displacement Results for 6th Degree of Freedom

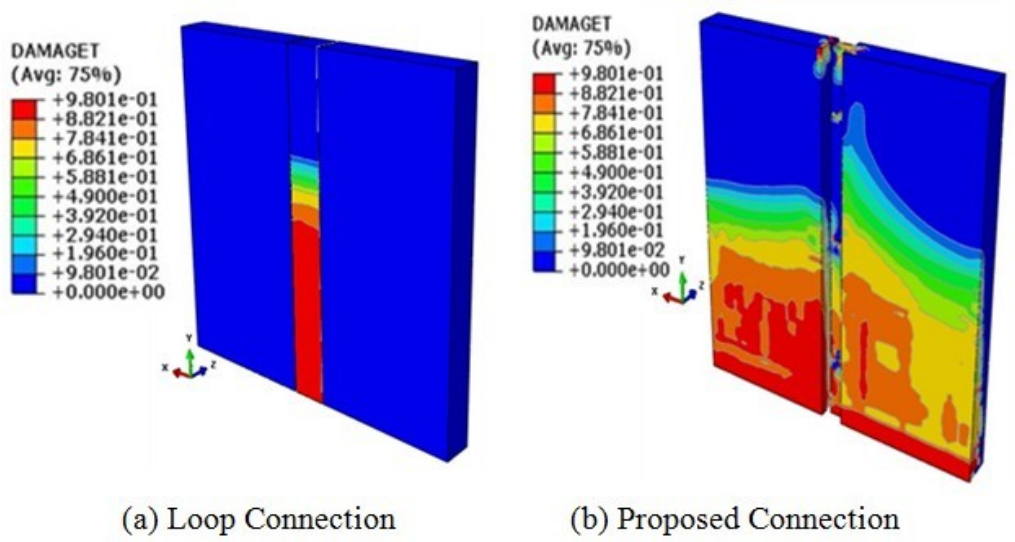

Fig. 25. DAMAGE-T Results for 4th Degree of Freedom

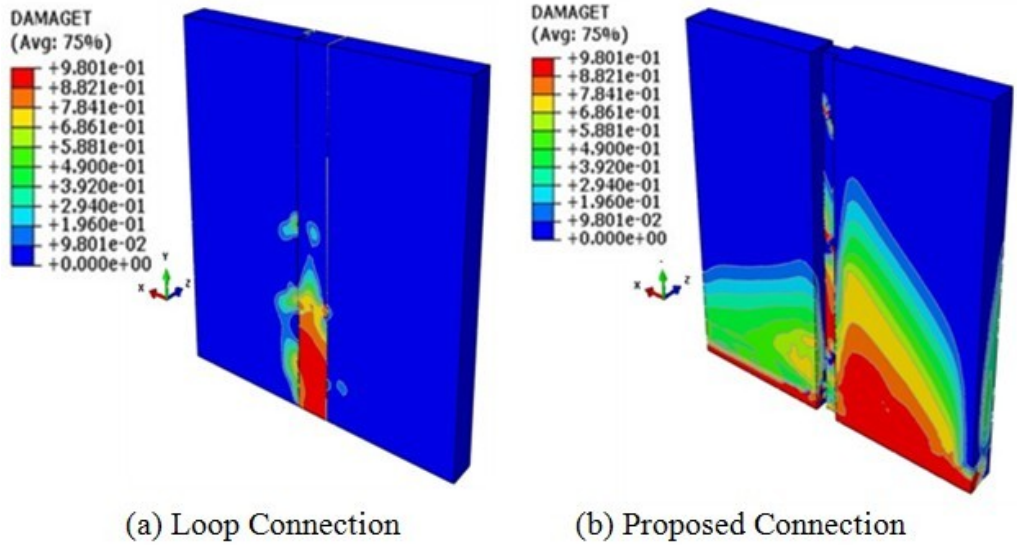

Fig. 26. DAMAGE-T Results for 5th Degree of Freedom

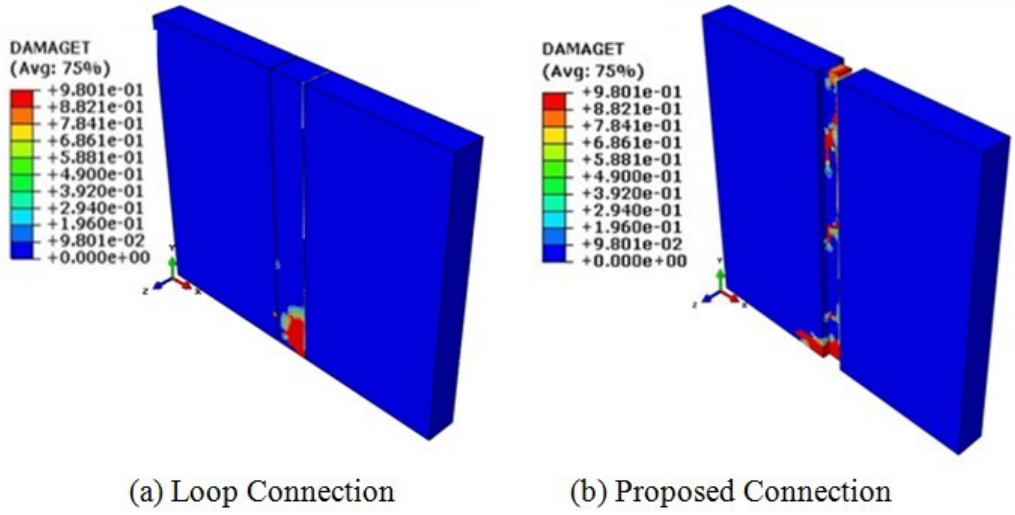

Fig. 27. DAMAGE-T Results for 6th Degree of Freedom

Based on the stress distribution and deformation results, it is concluded that the proposed connection shows better performance in terms of dissipating imposing force because of high damping rubber functioning. The results show that both aforementioned connections are in the plastic range for all three rotation DOFs. However, displacement of the right panel in the proposed connection is less than the corresponding value in the loop connection.

Cracks are propagated on the entire surface of precast walls in the proposed connection and show better distribution in comparison with the loop connection, in which cracks are formed near the connection subjected to monotonic loading in all three rotational DOFs.

Acknowledgements

This work received financial support from Housing Research Center of UPM and NAEIM Company and the supports are gratefully acknowledged.

References

1 **Nawi MM, Kamar K A M, Abdullah MR, Haron AT, Lee A, Arif M**, *Enhancement of Constructability Concept: An Experience in Offsite Malaysia Construction Industry*, In: Proceeding Changing Roles, New Roles: New Challenge Conference, Noordwick Aan Zee; the Netherlands, 2009.

2 **Yee AA**, *Social and Environmental Benefits of Precast Concrete Technology*, PCI journal, **46**(3), (2001), 14–19, DOI 10.15554/pcij.05012001.14.19.

3 **Institute AC**, *Guide to Emulating Cast-in-Place Detailing for Seismic Design of Precast Concrete Structures, Joint ACI-ASCE Committee 550*, American Concrete Institute, **ACI 550.1R-09**, (2009).

4 **Ericson AC**, *Emulative Detailing in Precast Concrete Systems*, In: Structures Congress 2010, 2010, pp. 2903–2913, DOI 10.1061/41130(369)262.

5 **Clough DP**, *Design of Connections for Precast Prestressed Concrete Buildings for the Effects of Earthquake*, PCI, 1986.

6 **Freedman S**, *Loadbearing Architectural Precast Concrete Wall Panels*, PCI Journal, **44**(5), (1999), 92–115, DOI 10.15554/pcij.09011999.92.115.

7 **Bhatt P, Kirk D**, *Tests on an Improved Beam Column Connection for Precast Concrete*, ACI Journal Proceedings, **82**(6), (1985), 834–843, DOI 10.14359/10395.

8 **Choi H-K, Choi Y-C, Choi C-S**, *Development and testing of precast concrete beam-to-column connections*, Engineering Structures, **56**(56), (2013), 1820–1835, DOI 10.1016/j.engstruct.2013.07.021.

9 **Khoo J-H, Li B, Yip W-K**, *Tests on precast concrete frames with connections constructed away from column faces*, 2006.

10 **Xue W, Yang X**, *Seismic tests of precast concrete, moment-resisting frames and connections*, PCI Journal, **55**(3), (2010), 102–121.

11 **Khaloo AR, Parastesh H**, *Cyclic loading of ductile precast concrete beam-column connection*, ACI Structural Journal, **100**(3), (2003), 291–296.

12 **Parastesh H, Hajirasouliha I, Ramezani R**, *A new ductile moment-resisting connection for precast concrete frames in seismic regions: An experimental investigation*, Engineering Structures, **70**(70), (2014), 144–157, DOI 10.1016/j.engstruct.2014.04.001.

13 **Naito C, Cao L, Peter W**, *Precast Concrete Double-tee Connections, Part I: Tension Behavior*, PCI Journal, **54**(1), (2009), 49–66.

14 **Cao L, Naito C**, *Precast concrete double-tee connectors, part 2: Shear behavior*, PCI Journal, **54**(2), (2009), 97–115, DOI 10.15554/pcij.03012009.97.115.

15 **Blandón JJ, Rodríguez ME**, *Behavior of Connections and Floor Diaphragms in Seismic-Resisting Precast Concrete Buildings*, PCI Journal, **50**(2), (2005), 56–75, DOI 10.15554/pcij.03012005.56.75.

16 **Pincheira JA, Oliva MC, Zheng W**, *Behavior of Double-Tee Flange Connectors Subjected to In-Plane Monotonic and Reversed Cyclic Loads*, PCI Journal, **50**(6), (2005), 32–54, DOI 10.15554/pcij.11012005.32.54.

17 **Bournas DA, Negro P, Molina FJ**, *Pseudodynamic tests on a full-scale 3-storey precast concrete building: Behavior of the mechanical connections and floor diaphragms*, Engineering Structures, **57**(57), (2013), 609–627, DOI 10.1016/j.engstruct.2013.05.046.

18 **Foerster HR, Rizkalla SH, Heuvel JS**, *Behavior and Design of Shear Connections for Loadbearing Wall Panels*, PCI Journal, **34**(1), (1989), 102–119, DOI 10.15554/pcij.01011989.102.119.

19 **Shultz A, Magana R, Trados M, Huo X**, *Experimental study of joint connections in precast concrete walls*, In: 5th US National Conference on Earthquake Engineering; Chicago, IL, USA, 1994.

20 **Bora C, Oliva MG, Nakaki SD, Becker R**, *Development of a precast concrete shear-wall system requiring special code acceptance*, PCI Journal, **52**(1), (2007), 122–135.

21 **Biondini F, Dal Lago B, Toniolo G**, *Seismic behaviour of precast buildings with cladding panels*, In: 15th World Conference on Earthquake Engineering (15WCEE); Lisbon, Portugal, 2012.

22 **Pantelides CP, Reaveley LD, McMullin PW**, *Design of CFRP composite connector for precast concrete elements*, Journal of Reinforced Plastics and Composites, **22**(15), (2003), 1335–1351, DOI 10.1177/073168403035581.

23 **Holden T, Restrepo J, Mander JB**, *Seismic Performance of Precast Reinforced and Prestressed Concrete Walls*, Journal of Structural Engineering, **129**(3), (2003), 286–296, DOI 10.1061/(ASCE)0733-9445(2003)129:3(286).

24 **Pennucci D, Calvi G M, Sullivan T J**, *Displacement-Based Design of Precast Walls with Additional Dampers*, Journal of Earthquake Engineering, **13**(S1), (2009), 40-65, DOI 10.1080/13632460902813265.

25 **Smith BJ, Kurama YC**, *Design of Hybrid Precast Concrete Walls for Seismic Regions*, ASCE 2009 Structures Congress, In: Structures Congress 2009, 2009, DOI 10.1061/41031(341)184.

26 **Biondini F, Dal Lago B, Toniolo G**, *Role of wall panel connections on the seismic performance of precast structures*, Bulletin of Earthquake Engineering, **11**(4), (2013), 1061–1081, DOI 10.1007/s10518-012-9418-z.

27 **Negro P, Bournas DA, Molina FJ**, *Pseudodynamic tests on a full-scale 3-storey precast concrete building: Global response*, Engineering Structures, **57**(57), (2013), 594–608, DOI 10.1016/j.engstruct.2013.05.047.

28 **Chakrabarti S, Nayak G, Paul D**, *Shear Characteristics of Cast-In-Place Vertical Joints in Story-High Precast Wall Assembly*, ACI Structural Journal, **85**(1), (1988), 30–45, DOI 10.14359/2965.

29 **Jansson PO**, *Evaluation of Grout-Filled Mechanical Splices for Precast Concrete Construction*, 2008.

30 **Ong KCG, Hao JB, Paramasivam P**, *Flexural behavior of precast joints with horizontal loop connections*, ACI Structural Journal, **103**(5), (2006), 664–671, DOI 10.14359/16918.

31 **Ong KCG, Hao J, Paramasivam P**, *Flexural Behavior of Precast Joints with Horizontal Loop Connections*, ACI Structural Journal, **103**(5), (2006), 664–671, DOI 10.14359/16918.

32 **Araújo DdL, Curado MC, Rodrigues PF**, *Loop connection with fibre-reinforced precast concrete components in tension*, Engineering Structures, **72**(72), (2014), 140–151, DOI 10.1016/j.engstruct.2014.04.032.

33 **Rossley N, Aziz AA, Nora F, Chew HC, Farzadnia N**, *Behaviour of Vertical Loop Bar Connection in Precast Wall Subjected To Shear Load*, Australian Journal of Basic & Applied Sciences, **8**(1), (2014).

34 **Jankowiak T, Lodygowski T**, *Identification of parameters of concrete damage plasticity constitutive model*, Foundations of Civil and Environmental Engineering, **6**, (2005), 53–69.